Integrated Nanophotonic Excitation and Detection of Fluorescent Microparticles

Sarp Kerman[1,2], Dries Vercruysse[1], Tom Claes[1], Andim Stassen[1, 2], Md. Mahmud ul Hasan[1,2], Pieter Neutens[1], Vignesh Mukund[1,2], Niels Verellen[1,2], Xavier Rottenberg[1], Liesbet Lagae[1,2], Pol Van Dorpe[1,2]

[1]imec, Kapeldreef 75, Leuven, B3001, Belgium

[2] Department of Physics and Astronomy, KU Leuven, Celestijnenlaan 200D, 3001 Leuven, Belgium

KEYWORDS: Integrated photonics, Silicon Nitride, Fluorescence, Focusing, Grating, Diffraction, On-chip, Detection, Lab-on-Chip, Point-of-Care, Cytometry

Table of Contents

S1. Phase Matching Design of Focusing Grating Couplers

The light was injected into a slab waveguide by a single mode waveguide. The light propagating in the slab hits the grating lines that are formed according to the phase matching condition. The scattered waves from each groove focus at the spot (f_x, f_z). For the ease of design, the focal spot is selected to be in the same vertical plane as the middle of the single mode waveguide ($f_y = 0$).

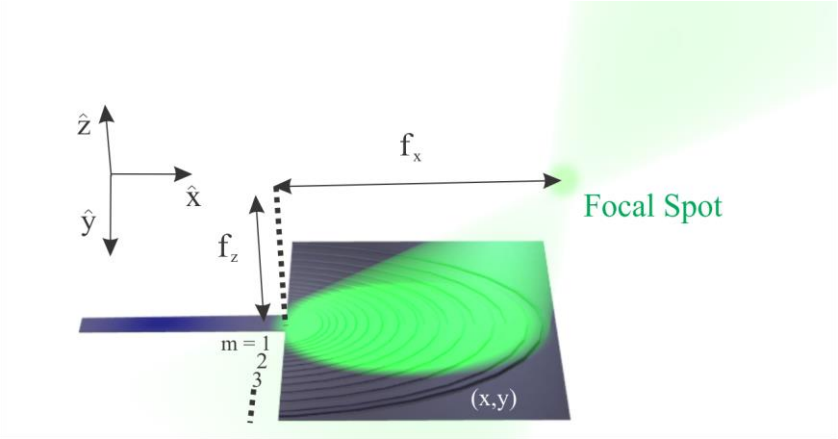

Figure S-1 . The phase matching design of the Focusing Grating Couplers.

The origin point is selected to be where the first scattering occurs. It is the junction between the single mode waveguide and the planar waveguide ($x_0 = 0, y_0 = 0$). The wave generated from this point must have a phase in the focal spot (f_x, f_z) that matches with the other waves scattered from the grooves at the position (x, y). Each groove line is drawn by orders of the integer $m = 1, 2, 3 \ldots$. Therefore, the phase matching equation can be derived as:

$$\frac{2\pi}{\lambda}\left[n_m\sqrt{f_x^2 + f_z^2}\right] + 2\pi m$$
$$= \frac{2\pi}{\lambda}\left[n_{eff}\sqrt{x^2 + y^2} + n_m\sqrt{(f_x - x)^2 + (f_y - y)^2 + f_z^2}\right] \qquad \text{(Eq. 1)}$$

Where λ is the wavelength, n_m is the refractive index of the medium above the sample, n_{eff} is the effective refractive index of the propagating mode in the planar waveguide, m=1,2,3.. is a positive integer and, x and y indicate the position of the groove corresponding to the integer m. The phase matching equation, Eq. 1, can be solved numerically. The corresponding points (x, y) form an elliptical line as shown in Fig. S-1.

S2. The Design of the Focusing Grating Coupler Platform for Fluorescence Excitation and Collection

The excitation and collection signals were routed by 400 nm wide single mode SiN waveguides. All FGCs were designed for the medium water and the SiN refractive index $n_{SiN} = 2.0$. They were modeled for 110 nm etch depth and the duty cycle 0.5. Their origins were defined as the middle of the single mode waveguides in y axis and where it was connected to the planar waveguide in x axis. In z axis, it was defined as the SiN top surface. The excitation FGC (FGC_E) was designed to focus at $f_x = 20\,\mu m$ and $f_z = 11\,\mu m$ away from its origin for the wavelength 633 nm with TE polarization. The in-line collection FGC, FGC_{CM}, was anticipated to focus at the same position. It was designed to focus at $f_x = 20\,\mu m$ and $f_z = 11\,\mu m$ away from its origin for the wavelength 657 nm with TE polarization. The side collection FGCs (FGC_{CL} and FGC_{CR}) were aimed to focus near the same position. Their origin was 30 µm away from the origin in y axis. They were anticipated to focus at $f_x = 20\,\mu m$ and $f_z = 11\,\mu m$ away from their corresponding origin for the wavelength 657 nm with TE polarization.

The linear grating couplers for out-coupling into the camera were placed on the waveguides. They were modeled for out-coupling the maximum fluorescence light to the angle within 30º with the surface normal. A 1µm SiO_2 top cladding and water medium was considered for modelling. The linear grating out-couplers consisted of 100 grooves, which were etched 220 nm. The period and the duty cycle was 620 nm and 0.5 respectively.

The FGC platform used for the photo-multiplier tube (PMT) detection had only the in-line collection FGC (FGC_{CM}). Fig. S-2 shows a bright field image of the platform.

Figure S-2. | Bright field image of the FGC platform used for PMT detection.

The collection single mode waveguide to be used for the experiments with the photo-multiplier tube (PMT) was routed for around 2 cm after FGC_{CM}. The single mode waveguide was extended to 10.0 µm width along a 100.0 µm propagation. A linear grating out-coupler was positioned after this extension. The grating coupler was designed to out-couple the light with the wavelength 657 nm to the angle 10º with the

normal. Water medium and a 1 μm SiO_2 top cladding were considered for modelling. The linear grating couplers consisted of 60 grooves, which were etched 220 nm deep with period 447 nm and duty cycle 0.59.

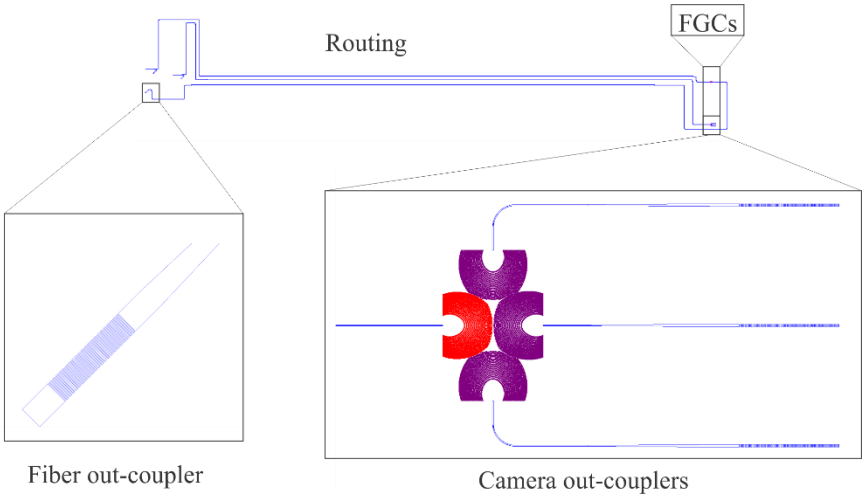

Figure S-3. The top view of the routing elements and the out-couplers.

S3. The Integration of the Microfluidic Channels

The microfluidic channels were designed to achieve sheet flow focusing. The sheet flow focusing provides the control of the confinement of the particle position in the microchannel. There were three inlet channels as displayed by the numbers 1,2 and 3 in Fig. S-4. A focused particle flow can be achieved by injecting the sample with particles in channel 2 while injecting additional medium in channels 1 and 3. The microchannel width was 300 μm after the junction.

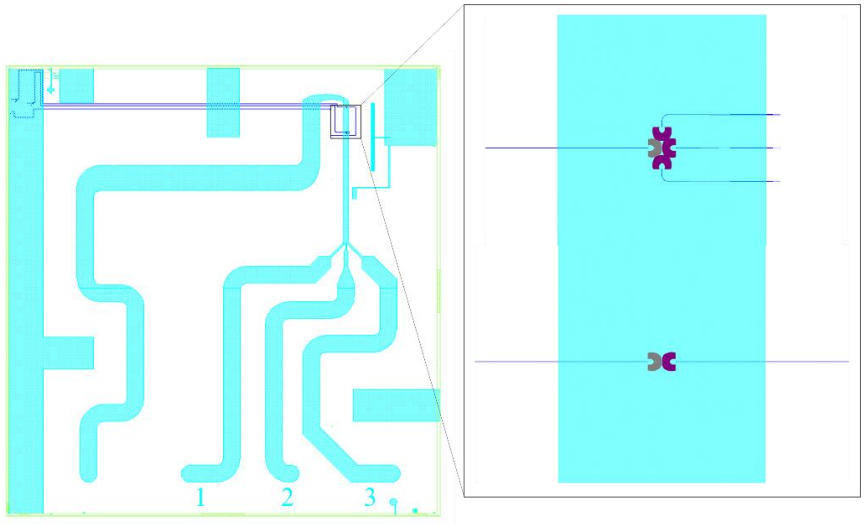

Figure S-4 . The microfluidic channel integration on the FGC platforms.

S4. FDTD Simulations of the Fluorescence Collection Efficiency

The 3D FDTD simulations were performed to characterize the fluorescence collection efficiency and the system collection efficiency of the in-line and side collection FGCs. Firstly, the reciprocity of the platform was used to calculate the fluorescence collection efficiency. A fundamental TE mode source was placed on the collection waveguide and excited the FGC. The field above the collection FGC was mapped. The simulation was performed for TE and TM polarized sources as the fluorescence can couple into both polarizations. The map was calibrated by a series of dipole simulations. A dipole source with varying polarizations was positioned above the FGC platform to measure the coupling into TE and TM polarization of the collection waveguide. The polarization of the dipole (TE and TM) was defined according to the orientation of the waveguide. The amplitude of the map that was obtained by the reciprocal approach was calibrated by the collection efficiency for the corresponding dipole position for different polarization coupling components (i.e. from dipole to-waveguide: TE-to-TE, TE-to-TM). An initial map was created by averaging the coupling map over TE-to-TE, TE-to-TM, TM-to-TM and TM-to-TM components. The TE components of the dipole (TE-to-TE and TE-to-TM) were averaged. And, separately the same was done for the TM components of the dipole (TM-to-TM and TM-to-TE). Secondly, the TE and TM maps were averaged by a weighing factor of TE:TM = 1:2; as TM polarization had two components while TE had one. The resulting map still contained the full spectral information. The weighted average of the map over the emission spectrum was calculated. The weight for each wavelength was taken as their fluorescence emission power. The fluorescence emission spectra of Crimson and Vybrant DiD dye were used. The resulting collection efficiency map shows how much of the fluorescence emitted by a point source can be coupled into the single mode waveguide which was defined as the fluorescence collection efficiency.

The system collection efficiencies for varying size of particles were analyzed for the collection peak position. For the 1 μm and 15 μm particles, the Crimson dye spectrum was used to calculate the collection efficiency map while the Vybrant DiD dye emission spectrum was used for the 5 μm particles (for PBMCs). It was assumed that the particles' refractive indices are close to water's and they don't significantly influence the excitation and collection profiles.

Firstly, the ratio of the light that is coupling in through the FGC and coupling out from the output grating coupler into the objective was calculated. For this, the spectral map that was obtained before the weighted averaging over the emission spectrum was multiplied by the out-coupling response of the linear grating coupler for each wavelength in the emission spectrum. The resulting map was multiplied by the excitation map to quantify how much of the excited fluorescence is collected and out-coupled into the objective. The resulting map was integrated over a spherical volume with the size of the particle. This value was divided by the integration of the excitation profile over the same region to obtain the ratio of the fluorescence that is excited,

collected and out-coupled to the total excited fluorescence. The resulting value was divided by the ratio of fluorescence collected by a water immersion objective (NA =0.8). It results in the system collection efficiency of the FGC.

S5. FDTD Simulations of the Particle Fluorescence Detection and Collection Efficiency for Mobile Particles

The particle fluorescence detection and collection efficiency for mobile particles are studied by the FDTD simulations. The particles are always mobile during the experiments. They can pass through the different regions of the excitation and collection beam paths during one integration time of a detector imaging the platform. The observed system collection efficiency depends on the position as well as the velocity of the particle and the integration time of the detector. The particles studied before were assumed to pass through the platform across the y-axis, in a duration shorter than a single integration time of the detector. By this assumption, the moving spherical particles can be considered as cylindrical with the long axis lying on the direction of flow: y-axis. The cylinder diameter is the same as the spherical particle diameter and the length of the cylinder depends both on the integration time of the detector and the velocity of the particle. The analysis was performed for the cylinders with the diameter 1 µm, 5 µm and 15 µm as done for the particles with the same diameters. The length of the cylinder was assumed to cover the entire simulation region in y-axis.

The amplitude of the collected signal depends on the lateral and vertical position of the particle. A detection efficiency was defined to evaluate the amplitude of the collected signal vs the position of a mobile particle as described before. The detection efficiency was calculated by integrating the multiplication of the excitation map and collection efficiency map over the cylindrical region.

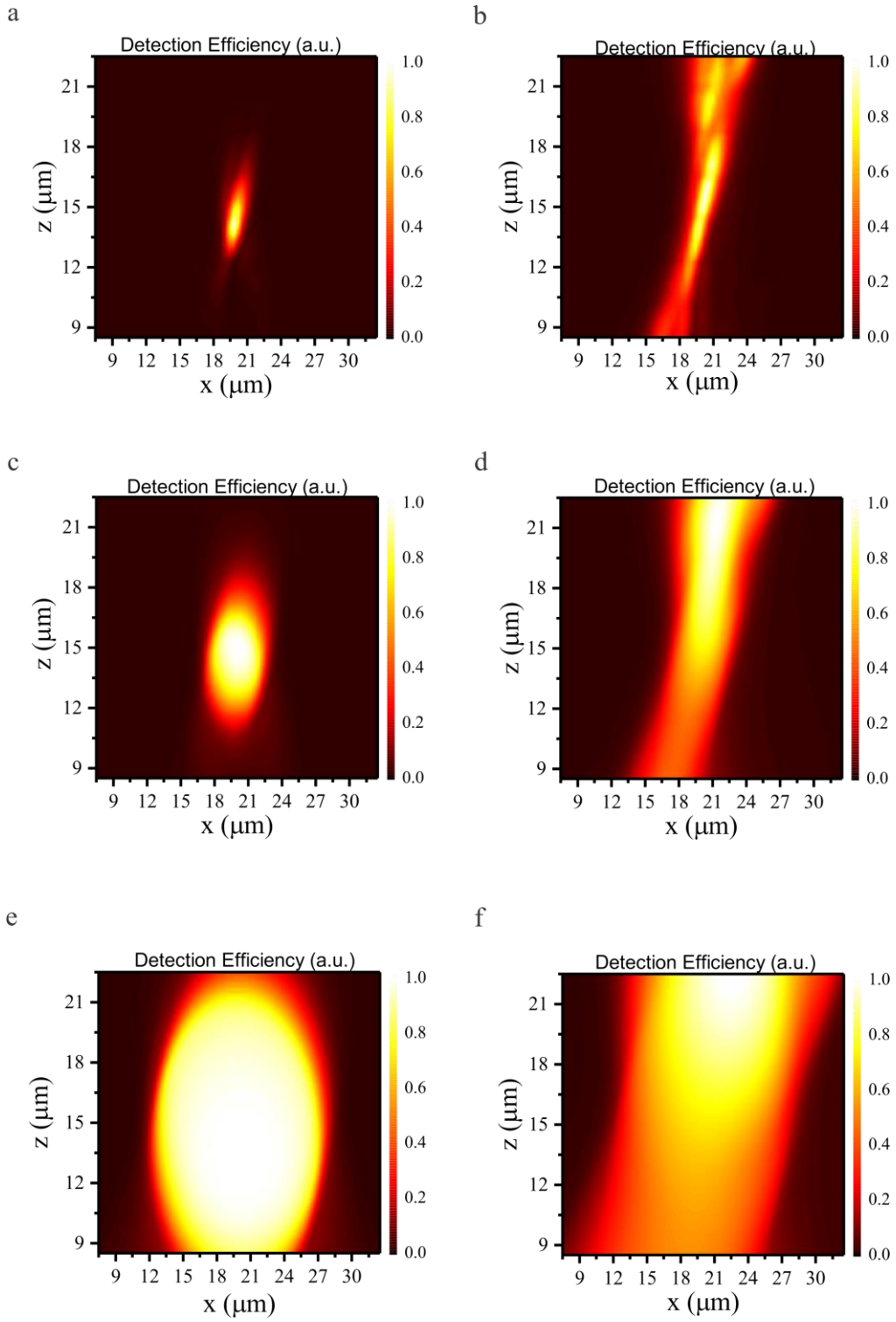

Figure S-5. The FDTD simulation results of the detection efficiency of a mobile 1 μm particle for FGC_{CM} (a) and FGC_{CR} (b), 5 μm particle for FGC_{CM} (c) and FGC_{CR} (d) and 15 μm particle for FGC_{CM} (e) and FGC_{CR} (f).

Fig. S-5 shows the fluorescence detection efficiency of mobile particles with the diameter of the 1 μm, 5 μm and 15 μm particles for FGC_{CM} and FGC_{CR} for varying position. It was observed that the detection region becomes wider and more uniform as the particle gets larger. For FGC_{CM}, a 15 μm particle can result in nearly the same amplitude of signal within a circular region in the x-z plane with the diameter nearly 10 μm. However, the diameter of this circular region is only around 2 μm for a 1 μm particle. The detection efficiency decays rapidly away from this circular region. Therefore, the detection of 1 μm particles highly depends on their lateral and vertical position. The same trend of broadening of the detection region with the increasing particle size could also be observed for FGC_{CR}. For the 5 μm and 15 μm particles, the maximum detection for FGC_{CR} occurs at a location approximately 7 μm away from the one for FGC_{CM}. However, the region is broad enough to allow simultaneous detection by FGC_{CM} and FGC_{CR} for those particles. On the other hand, the maximum detection of 1 μm particles for both the symmetric and side FGCs take place at the same position. This region is comparable to the particle size as mentioned before. The detection efficiency profile of FGC_{CR} covers a broader region and has multiple local peaks. Therefore, the simultaneous detection of 1 μm particles by the symmetric and the side FGCs is highly unlikely.

S6. The Focal Position of FGCs for Varying Wavelength

The position of the focus formed by FGC_{CM} was experimentally analyzed from 600 nm to 710 nm. Fig. S-6 depicts the position dependency of the focus on the wavelength. The focus became closer to the origin (x_0 = 40 μm, z_0 = 0 μm) of the grating both in the horizontal and vertical axis as the wavelength increased. The shift was linearly proportional to the wavelength variation. The shift in x and z axis per unit wavelength was 27.42 μm/ μm(wavelength) and -30.50 μm/ μm(wavelength), respectively.

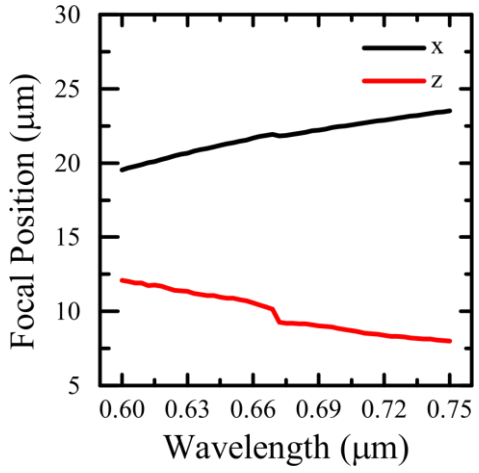

Figure S-6. The experimental focal position of FGC_{CM} for varying wavelength.

S7. Fluorescence Collection by The Symmetric Collection Focusing Grating Coupler

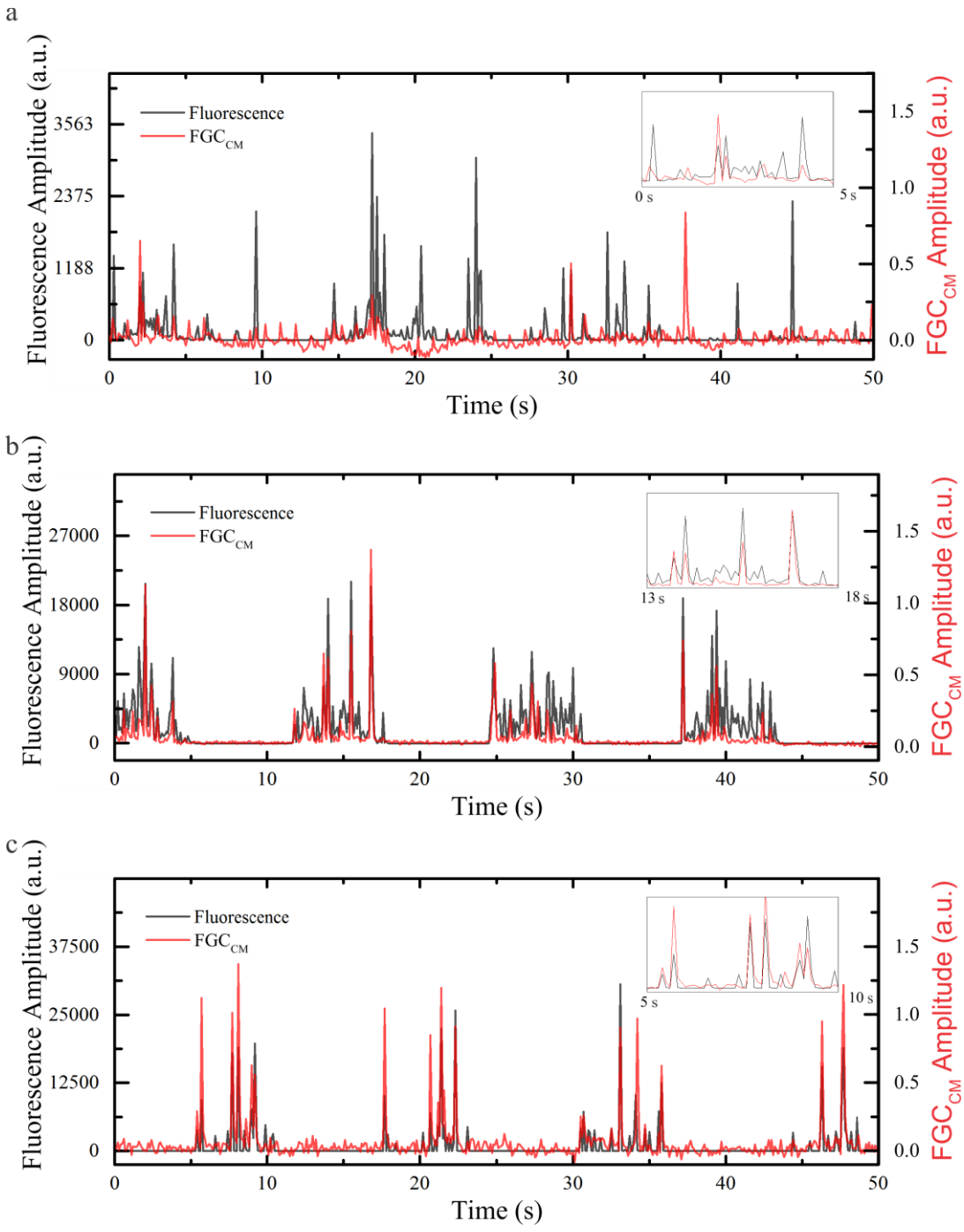

Figure S-7 . The amplitude of the fluorescence signal from the particle and the linear out-coupler of the symmetric collection FGC as a function of time for 1 µm polystyrene particles (a), PBMCs (b) and 15 µm polystyrene particles (c).

S8. Fluorescence Collection by The Side Collection Focusing Grating Couplers

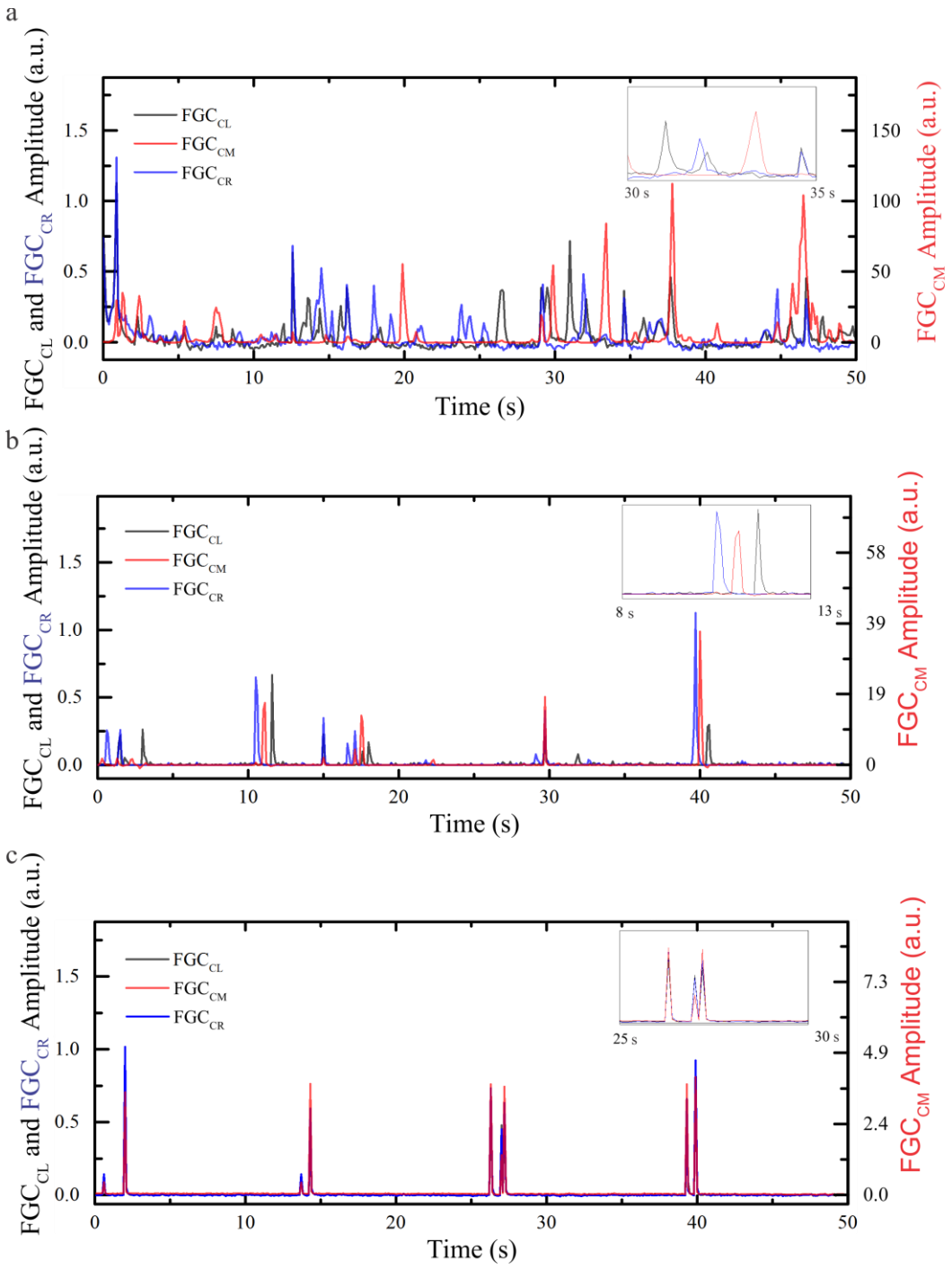

Figure S-8. The amplitude of the fluorescence signal from the linear out-coupler of $FGC_{CL,}$ FGC_{CR} and FGC_{CM} as a function of time for 1 µm polystyrene particles (a), PBMCs (b) and 15 µm polystyrene particles (c).

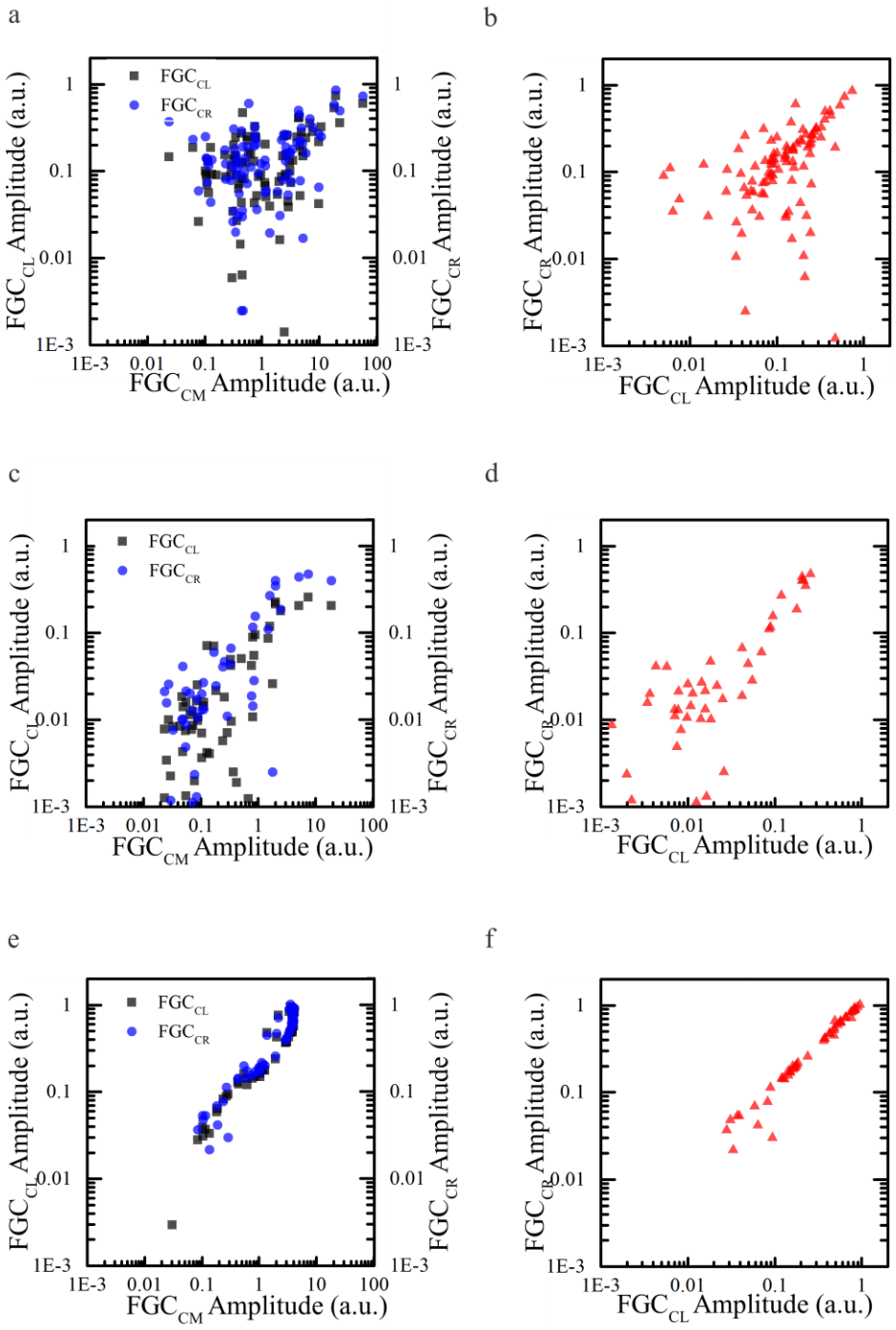

Figure S-9. The amplitude of each event from FGC_{CL} and FGC_{CR} compared to FGC_{CM} for 1 µm polystyrene particles (a), PBMCs (c) and 15 µm polystyrene particles (e), and the comparison of amplitude of each event from FGC_{CL} and FGC_{CR} for 1 µm polystyrene particles (b), PBMCs (d) and 15 µm polystyrene particles (f).

S9. Fluorescence Detection by Photo Multiplier Tube

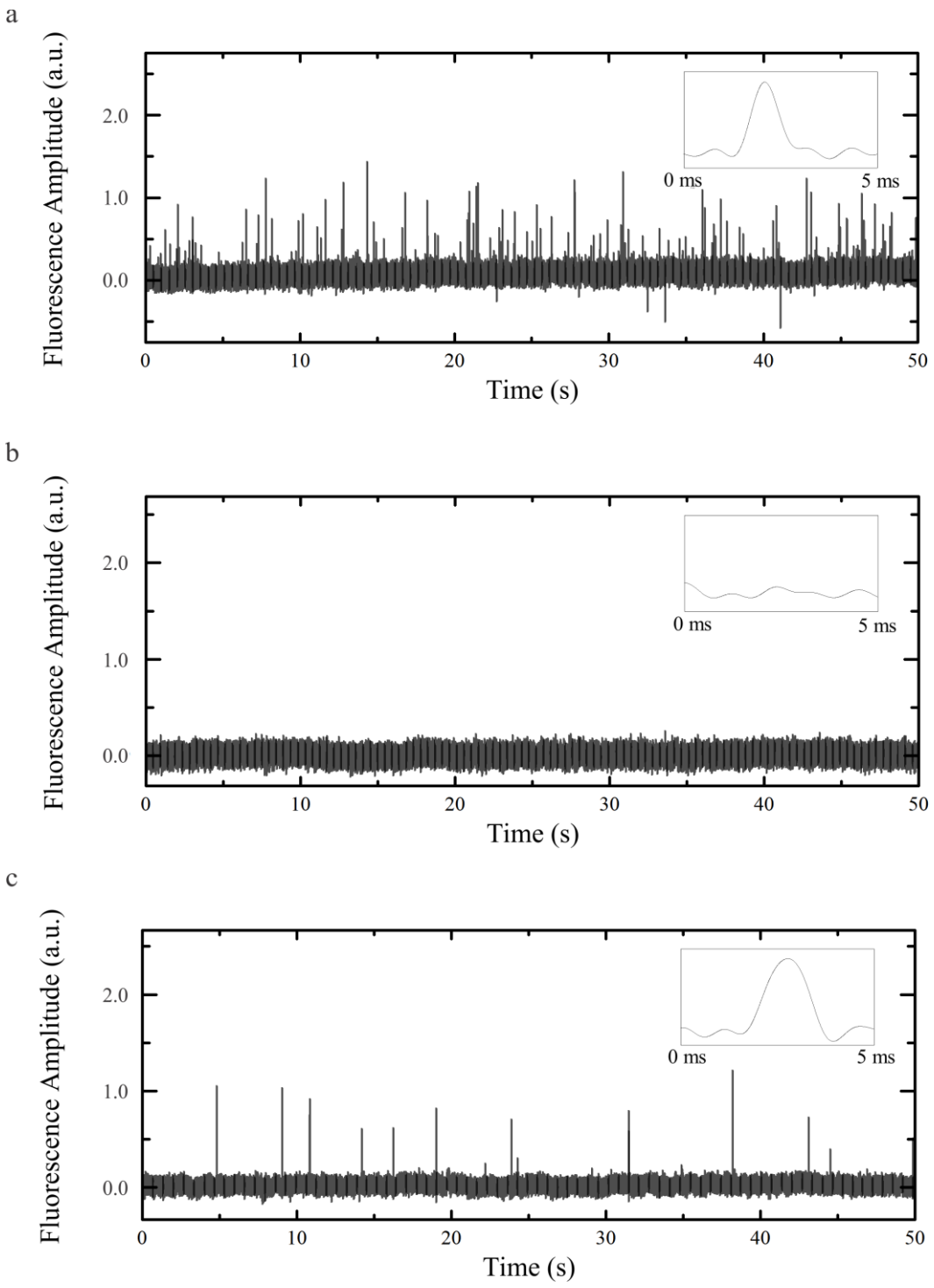

Figure S-10. The amplitude of the fluorescence signal from the PMT as a function of time for 1 µm polystyrene particles (a), PBMCs (b) and 15 µm polystyrene particles (c).

S10.Methods

Fabrication

The fabrication of the SiN FGC samples has been done in the imec pilot line facilities. Firstly, 80 nm SiN was deposited by plasma-enhanced chemical vapor deposition (PECVD) on the 200 mm Si wafer as an anti-reflection layer. A 2.3 µm bottom cladding SiO2 layer was deposited on top of the anti-reflection layer by PECVD. The roughness upon this deposition was reduced by chemical-mechanical planarization (CMP). This process also took away 100 nm SiO_2. 100 nm SiO_2 was deposited by high density plasma deposition (HDP) to reach 2.3 µm bottom cladding thickness. The waveguide layer, 220 nm SiN, was deposited by PECVD on top of the bottom cladding layer. Using 193 nm deep-ultraviolet lithography (DUV), the input grating and focusing grating couplers were patterned on the SiN layer and subsequently were dry etched to a depth of 110 nm. In a second DUV step the SiN waveguides were patterned and again dry etched to the full depth (220 nm) to form 4 µm wide trenches on both sides of the waveguide. The roughness of the top cladding was reduced by CMP and finally, a 1 µm top bottom cladding SiO2 was deposited on top.

The second step was the fabrication of the microfluidic channels on top of the SiN FGC platform. Firstly, the PA layer was spin coated on top of the chip. The microfluidic channels and the input/output grating couplers were opened by the photolithoghraphy on the PA layer.

The 200 mm wafer has been diced into samples in dimensions 25740x26700 µm. Finally, the microfluidic channels were finally closed by sealing the chip with a glass slide. The glass slides were bonded to the PA layer by thermal compressive bonding at 200 ºC for 30 seconds.

Particles

The fluorescence excitation and collection was tested by the 1 µm and 15 µm polystyrene particles with Crimson dye and PBMCs with Vybrant DiD dye. The polystyrene particles were commercial FluoSpheres® Polystyrene Microspheres from ThermoFischer Scientific. The concentrations of the 1 µm and 15 µm particles were $1x10^9$ beads/mL and $2x10^5$ beads/mL for the microscopy experiments. For the photo-multiplier tube (PMT) experiments, $1x10^6$ beads/mL of 15 µm particles was used.

PBMC preparation has started from the whole blood from healthy volunteers. It was poured into BD Vacutainer® tubes (4 mL, K3-EDTA, Becton Dickinson) and subsequently diluted 1:1 with phosphate buffered silane (PBS). 4 mL diluted blood samples were layered over 3 mL Ficoll-Paque PLUS (GE Healthcare). The solution was centrifuged in a horizontal rotor 400xg for 35 minutes, according to the manufacturer's instructions. The PBMC fraction was collected and washed to remove contaminating platelets. It was re-suspended in PBS supplemented with 0.5% bovin serum albumin (BSA) and 2 mM Ethylenediaminetetraacetic acid (EDTA). The PBMC fraction was suspended in 1 mL of PBS buffer at a density of ~$1x10^6$ cells/mL. 5 µl of Vybrant® DiD Cell-Labeling solution (ThermoFisher Scientific) was added and the sample was incubated at 37°C in the dark for 30 minutes. The labeled cell suspension was subsequently washed twice and re-suspended in PBS supplemented with 0.5% BSA and 2 mM EDTA for later measurements.

FGC Focus and Power Characterization Measurements:

A confocal microscope with a spectrometer was utilized for mapping the intensity of the light coming out of the FGCs for the characterization of the FGC platform. The light was generated by a supercontinuum laser source and guided by a single mode fiber. It was filtered for the desired wavelength range by an acousto-optic tunable filter. The light was injected into the single mode waveguide via input grating couplers to test the excitation FGC (FGC_E) for the wavelength 638 nm. The symmetric collection FGC (FGC_{CM}) was characterized by injecting the light through the output grating coupler of the platform. It was tested for the wavelength range between 600 and 750 nm.

The light coming out of the FGCs was collected by a 40x water immersion objective with the numerical aperture NA=0.8. The signal was carried into the spectrometer for the quantification of its amplitude to profile the beam path for different wavelengths. The sample was placed on a piezo stage for three dimensional scanning of the beam profile above the sample surface.

The power of the light in the focal point of the excitation FGC was characterized. The input laser power was adjusted to 31.8 mW. The power in the focus was measured by using a 63x (NA =1.40) oil immersion objective. It was focused on the focal spot of the FGC and the power was recorded by a power meter. Secondly, the power in the waveguide was measured by the same objective on a diced sample. The objective was focused onto the diced waveguide facet and the power after the objective was measured. The power in the waveguide and the focus were compared for the characterization.

Particle Fluorescence Excitation and Collection Measurements:

The microscopy experiments were performed by a diode laser at 638 nm. The light was guided by a single mode fiber and injected into the single (TE) mode waveguide via a linear input grating coupler at the side of the photonic/microfluidic chip. The particles were injected into the microfluidic channel 2 and additional medium (water) was injected in channels 1 and 3. (see Fig. S-3). The flow of the particles was focused into the middle of the channel by adjusting the pressure in each channel with a Fluigent microfluidic pump.

A 40x water immersion objective (NA = 0.8) was used to image the fluorescence from the particle and the three output linear grating couplers. A 638 ± 5 nm notch filter was used to remove the excitation light. A CCD camera was used with a 100 ms for all the measurements.

For the efficiency analysis of the middle collection FGC for 1 and 15 μm polystyrene particles, 1.07 mW fiber input power was used. 12.7 mW and 13.8 mW fiber input powers were injected for the efficiency analysis of the side collection FGCs for 15 μm and 1 μm polystyrene particles. 13.8 mW laser power was used for the analysis of both the middle and side collection FGCs for PBMCs.

The experiments performed with PMT were done by Photosensor module H10722-01 from Hamamtsu. The light was injected into the chip by a single mode fiber where the input power was kept at 0.16 mW for all the experiments.

1 μm and 15 μm polystyrene particles and PBMCs were used for the PMT experiments. The fluorescence was collected from the output single mode waveguide by a multimode fiber via a linear grating coupler. A long pass filter was used to block the excitation light after the multimode fiber. The multimode fiber was guided to the PMT. The PMT was operated at 500 kHz and the signal was filtered by a 10 kHz low pass filter to increase the signal to noise ratio.

FDTD Simulations

All simulations were performed with the commercial software Lumerical FDTD v8.6.3. A x×y×z=32×65×45μm space was simulated with 29x31x30 nm mesh. This mesh sized was observed to be sufficient after doing a mesh convergence test. In the simulation the Si substrate was ignored. The structure was simulated only considering the SiO_2 layer below and assuming water above, where the light focuses.